DOI: 10.1002/adma.200701899

Nanoporous Plasmonic Metamaterials**

By *Juergen Biener,* Gregory W. Nyce,* Andrea M. Hodge, Monika M. Biener, Alex V. Hamza,* and *Stefan A. Maier*

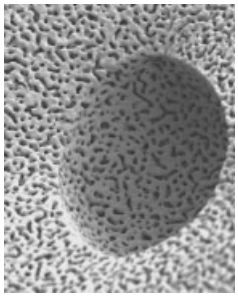

We review different routes for the generation of nanoporous metallic foams and films exhibiting well-defined pore size and short-range order. Dealloying and templating allows the generation of both 2D and 3D structures that promise a plasmonic response determined by material constituents and porosity. Viewed in the context of metamaterials, the ease of fabrication of samples covering macroscopic dimensions is highly promising, and suggests more in-depth investigations of the plasmonic and photonic properties of this material system for photonic applications.

1. Introduction

Research in plasmonics is driven by the desire to create materials with designed photonic properties taking advantage of electromagnetic resonances and concomitant enhancement of the electromagnetic near-field owing to localized surface plasmons.[1,2] In order to arrive at a macroscopic response, in general ordered arrays of plasmonic constituents such as metal nanoparticles are required.[3,4] Viewed in the concept of metamaterials,[5] the sub-wavelength periodicity of these structures results in an effective permittivity function. While many photonic applications require materials with well-developed long-range order which, for example, can be prepared by colloidal crystal-templating methods,[6] also disordered materials can exhibit useful photonic functions with effective permittivities governed by the underlying short-range order. In this regard, the development of nanoporous metallic materials for photonic and plasmonic applications has recently attracted much interest. For example, Yu et al. demonstrated excitation of both propagating and localized surface plasmon resonances in nanoporous gold membranes,[7] Dixon et al. reported surface plasmon resonances in ultra-thin films of supported nanoporous Au,[8] and Maaroof et al. showed that the plasmonic behavior of nanoporous gold films can be controlled by controlling the porosity.[9]

One of the main drivers for the development of plasmonic metamaterials by colloidal self-assembly or material growth processes is the desire to improve the sensitivity of surface enhanced Raman spectroscopy (SERS) for fundamental molecular science as well as sensor applications. In this context, the localized plasmon modes sustained by the material are responsible for the large field enhancement achieved on nanoporous metal surfaces.[10] Optimizing the plasmonic response of nanoporous metals requires the capability to fine-tune the feature size (specifically the size of the pores of the structure. Despite the fact that long-range order is not required for this application, most of the studies have been performed on periodic structures such as inverse opal crystals.[11,12] Here, we will provide a short review of the synthesis of non-periodic nanoporous metallic materials. In contrast to the periodic structures mentioned above, these materials are not limited to thin films, but can easily be prepared in the form of millimeter-sized 3D objects. Although these structures do not exhibit the long-range order of an

[*] Dr. J. Biener, Dr. G. W. Nyce, Dr. M. M. M. Biener, Dr. A. V. Hamza
Nanoscale Synthesis and Characterization Laboratory
Lawrence Livermore National Laboratory
Livermore, CA 94550 (USA)
E-mail: biener2@llnl.gov; nyce2@llnl.gov

Prof. A. M. Hodge
Aerospace and Mechanical Engineering Department
University of Southern California
Los Angeles, CA 90089 (USA)

Dr. S. A. Maier
Experimental Solid State Group, Department of Physics
Imperial College
London SW7 2AZ (UK)

[**] This work was performed under the auspices of the U.S. Department of Energy by Lawrence Livermore National Laboratory under Contract DE-AC52-07NA27344.

ADVANCED MATERIALS

inverse opal structure, they still have excellent short-range order and can be very uniform over large volumes. The techniques described in the following have been developed or improved at Lawrence Livermore National Laboratory with the ultimate goal to design a new class of 3D nanoporous metals for high energy density laser experiments. This application requires the fabrication of millimeter-sized, defect-free monolithic samples of nanoporous materials with well-defined pore-size distributions (including hierarchical porosities) and adjustable densities down to a few atomic percent. Besides sensor applications,[7,13] such materials have also very interesting catalytic[14–16] and mechanical properties.[17,18] Specifically, we will address top-down (e.g., dealloying) and bottom-up techniques (e.g., filter casting and templating) as well as combinations thereof. We also will review the optical properties of these materials so far they have been studied by us or other groups.

2. Dealloying

Among the top-down approaches dealloying is an extremely simple and flexible method. In metallurgy, dealloying is defined as selective corrosion (removal) of the less noble constituent from an alloy, usually via dissolving this component in a corrosive environment.[19] This process can lead to spontaneous pattern formation, that is, development of a 3D bicontinuous nanoporous structure while maintaining the original shape of the alloy sample. Thus, virtually any desired shape of the nanoporous material can be obtained by using an appropriately shaped alloy sample. A well-studied example is the

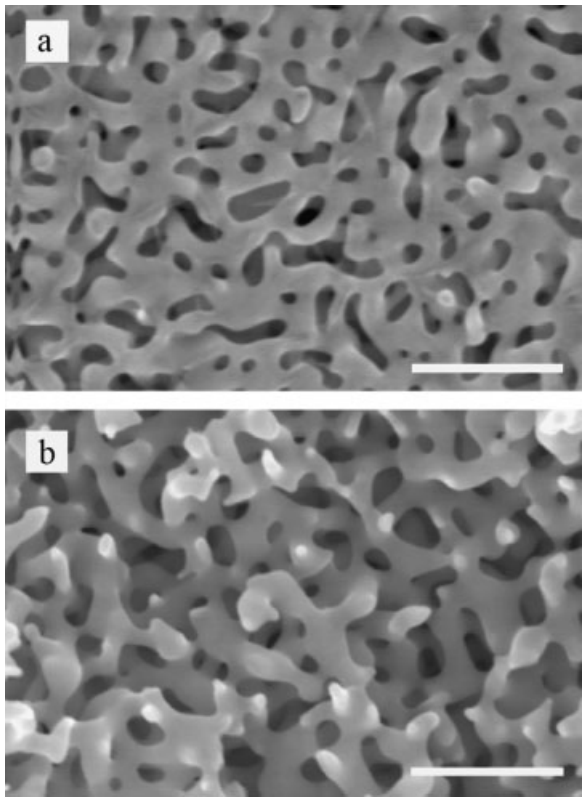

Figure 1. a) Plane-view, and b) cross-sectional scanning electron microscopy (SEM) images showing the characteristic spongelike open-cell foam morphology of np-Au. The material is very homogeneous and exhibits nanometer-sized pores and ligaments, the latter with a length-to-diameter aspect ratio close to one. The scale bars are 300 nm.

Dr. Juergen Biener was born 1961 in Augsburg, Germany. He studied chemistry at the Ludwig-Maximilians-Universität in Münich and conducted his doctoral research in the field of surface science at the Max-Planck-Institute of Plasma Physics (IPP) in Gärching. In 1997 he received a fellowship from the German Academic Exchange Service (DAAD) to work with Bob Madix at Stanford University, CA on metal oxide model catalysts. In 2000 he returned to the IPP to continue his research on plasma-wall interactions. In 2003 he accepted a visiting scientist position at the Center for Imaging and Mesoscale Structures at Harvard University, MA where he developed a new view of the reactivity of gold surfaces. Currently, he is one of the leaders in the Nanoscale Synthesis and Characterization Laboratory at the Lawrence Livermore National Laboratory. His research interest lies at the intersection of surface chemistry, physics, and mechanics of nanostructured materials.

Dr. Gregory Nyce was born and raised in Warrenton, VA. He attended Virginia Tech and received his B.Sc. in Biochemistry in 1995. His interest in organometallic chemistry led him to move to California to pursue his graduate work in lanthanide/actinide chemistry at the University of California, Irvine under the direction of William J. Evans. After receiving his Ph.D. in 2001, he moved to the San Francisco bay area to pursue a joint post-doc at IBM Almaden Research/Stanford University under the direction of Jim Hedrick and Robert Waymouth. At IBM/Stanford he helped to pioneer organic polymerization catalysis. In 2004, he accepted a staff scientist position at Lawrence Livermore National Laboratory (LLNL). At LLNL, he develops low-density inorganic and organic materials for the Nanoscale Synthesis and Characterization Lab.

formation of nanoporous gold (np-Au) via selective removal of Ag from a Au–Ag alloy.[20] In this system, the removal of silver can be achieved by simply submerging the alloy sample in concentrated nitric acid (so-called ''free corrosion'') or by applying an electrochemical driving force in a less corrosive electrolyte.[21] The process works best in a narrow compositional range around $Ag_{0.7}Au_{0.3}$,[22] and generates a material with a characteristic spongelike open-cell morphology and a uniform feature size on the nanometer length scale (Fig. 1). The specific surface area of the materials is in the order of a few $m^2\ g^{-1}$.[23] Pattern formation during dealloying seems to be a consequence of local surface passivation by clustering of Au adatoms in combination with continuous etching of Ag.[20] Within this simple model, the length scale of the structure should be a function of the diffusion length of clustering vacancies and Au adatoms, which are continuously generated during dealloying. This conclusion is consistent with the observation that the feature size in np-Au can be controlled by the composition of the electrolyte, which in turn controls the diffusion length.[24] For plasmonic applications it is important to note that the process can be easily extended to 2D films by using commercially available white gold leaf with a thickness of a few hundred nanometers.[25]

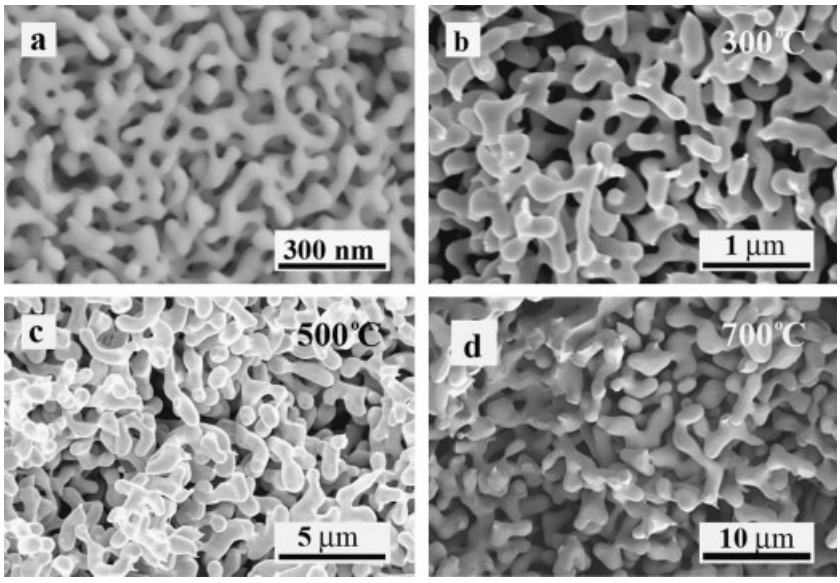

Figure 2. Cross-sectional SEM images of a) as-prepared and annealed np-Au at b) 300 °C, c) 500 °C, and d) 700 °C. Note the self-similarity of the structure while increasing the feature size by more than a factor of 30. The relative density of the materials remains constant at approximately 30%.

An equally important aspect of the dealloying process is that the feature size in nanoporous gold can be controlled over a wide range from 10 nm to the micrometer length scale through a simple annealing procedure. Most notably, this process does not affect the relative density or relative geometry of the material (ligament connectivity or ligament/pore/sample shape).[26,27] An example of such an annealing experiment is shown in Figure 2. Note the self-similarity of the structure while increasing the feature size by more than a factor of 30.

This effect can be used to fine-tune the optical properties of np-Au. For example, we were able to achieve SERS enhancement factors in the range of 10^9–10^{11} by tuning the average pore width of np-Au to ~250 nm.[13] The correlation between pore width and SERS response is shown in Figure 3. Our data also show that the SERS enhancement correlates better with the pore size than with the ligament width, consistent with findings from inverse opal structures.

Large SERS enhancement factors and size effects in the optical properties of np-Au prepared by dealloying have also been observed by other groups. For example, Dixon et al. studied the SERS response of supported thin films of np-Au, and reported enhancement factors of up to 10^4.[8] The observed SERS enhancement showed a complex dependence on the film thickness and dealloying time which both affect the morphology of the material. For example, the authors find that the

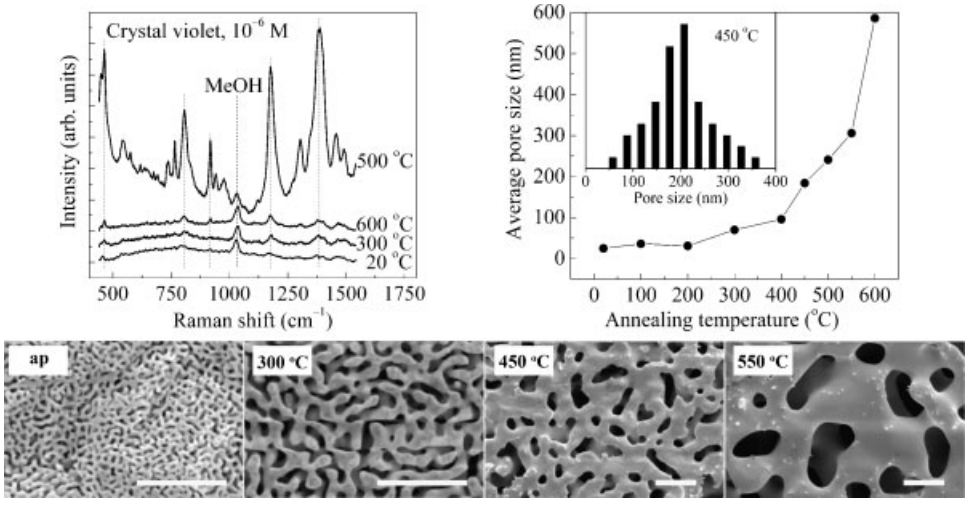

Figure 3. Left: SERS spectra (632.8 nm excitation) of a 10^{-6} *M* crystal violet/methanol solution as a function of the annealing temperature of np-Au. The methanol-related peak is labeled ''MeOH''. Lower panel: SEM images showing the evolution of the surface morphology as a function of annealing. The samples were annealed for 2 h at each temperature, and the scale bar is 1 μm in all images. Right: Dependence of the average pore width on annealing temperature. The inset shows the distribution of pore widths after annealing at 450 °C.

ADVANCED MATERIALS

onset of the SERS effect with increasing film thickness correlates with the appearance of a surface plasmon resonance feature in ellipsometric spectra. The opposite size effect, that is smaller pores provide stronger enhancements, has recently been reported by Qian et al.[28] Here, the authors argue that the observed SERS enhancement depends strongly on roughness of the ligament surface, and that different ligament nanostructures may be responsible for the different results. In our point of view, it is the actual pore/sample surface shape which controls the SERS response. This brief summary of the available data regarding the SERS response of np-Au prepared by dealloying clearly demonstrates the necessity of future studies addressing the structure-property relationship of these materials. Here, the development of techniques for pore size control should be of great value for separating plasmonic (i.e., field confinement related to pore size and shape) and static (lightning-rod) effects. But regardless of the details, np-Au is a unique optical material in that it supports both propagating and localized surface plasmon resonances as recently demonstrated by Yu et al.[7]

The dealloying technique can also be used to introduce more complicated morphologies such as hierarchical porosities by using ternary alloys such as Cu–Ag–Au as starting material. The idea is the following: First, the least noble metal is removed thereby creating a nanoporous binary alloy sample. In a second step the material is annealed to the desired feature size. Finally, nanometer-scale porosity is reintroduced into the ligaments of the structure by removing the second component of the original ternary alloy system (in this example Ag). We have successfully used this technique to prepare low-density (~10 at % relative density) np-Au samples with bimodal pore size distributions. The main challenge of this approach is the making of a homogeneous single phase starting alloy which is extremely challenging due to a miscibility gap in the ternary Cu–Ag–Au phase diagram. In general, the step-wise dealloying approach outlined above is severely limited by the availability of suitable ternary alloys. In the case of thin film samples, Ding and Erlebacher were able to overcome this limitation by developing a novel gas-phase electroless Ag plating technique.[29] The trick is to redeposit Ag on the coarsened ligament structure of annealed nanoporous Au followed by a second dealloying step. Using this two-step dealloying/Ag plating strategy, Ding and Erlebacher successfully fabricated ultrathin gold membranes with bimodal pore size distributions.[29]

3. Templating

Besides dealloying, templating is another approach to incorporate and control porosity.[6,30–33] Here sacrificial inorganic or organic materials are used as templates to generate a nanostructured porous solid. In particular, the combination of templating and dealloying techniques provides a powerful approach to create materials with complex hierarchical porosities.[34] In the following, some typical examples of the fabrication of nanoporous gold foams based on templating techniques will be described (Scheme 1). The synthesis always starts with the preparation of Au or Ag–Au coated core/shell particles. After assembling (casting) these into a monolithic porous structure, a pure metal foam can be obtained by removing the core material (template). In the case of Ag–Au foams a dealloying step can be added to create hierarchical porosities.

Hollow Ag/Au shells can be fabricated by using silica[35] or polystyrene[36–38] spheres as templates. For our application, polystyrene (PS) is clearly the preferred choice as micro beads with a narrow size distribution are readily available. PS templates can also be easily removed at elevated temperatures or by dissolution in an appropriate organic solvent. Furthermore, PS beads can be metal coated by employing simple electroless plating methods.[37] For the application described here one would typically use PS beads with a diameter ranging from a few hundred nanometers to several micrometers. The challenge is to prepare the large quantities of metal-coated spheres needed for the fabrication of millimeter-sized foam samples. This makes it necessary to work with highly concentrated solutions of PS beads that are prone to particle aggregation,[39] which in turn negatively affects the subsequent casting process. However, highly concentrated colloidal suspensions of PS beads can be stabilized by adding a polymer stabilizer such as polyvinylpyrrolidinone (PVP) to the plating bath. Using this approach we were able to coat large quantities of PS beads with Au films of homogeneous thickness and little apparent particle aggregation. Finally, the metal-coated PS beads are isolated and redispersed in distilled water.

The next process step is casting to obtain a monolithic nanoporous sample. The procedure is analogous to slip-casting of ceramic[40] and metal[41] particles in which a suspension of particles is poured into a tube inserted into plaster of paris

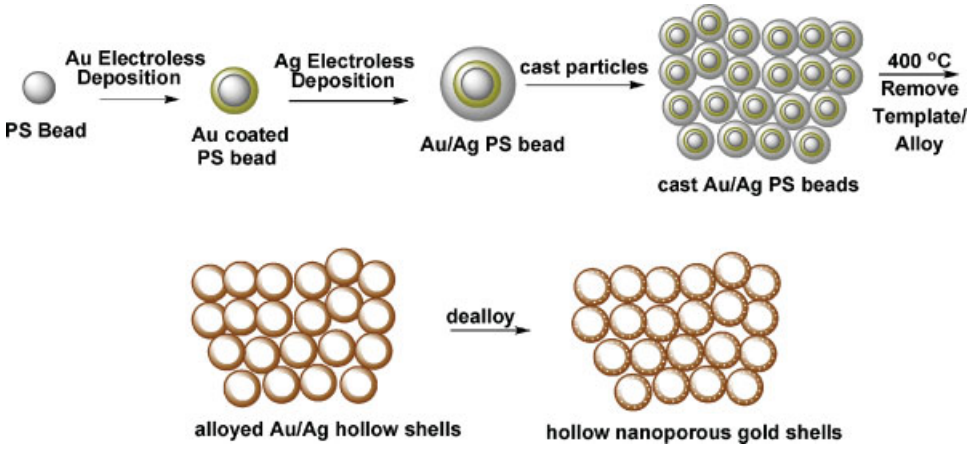

Scheme 1. Synthesis of low-density gold monoliths comprising nanoporous hollow gold shells.

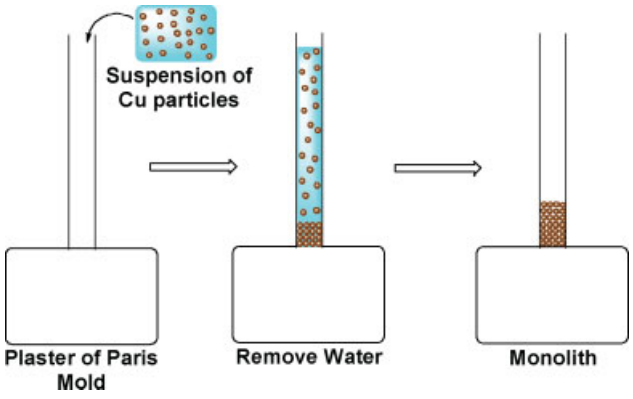

Scheme 2. Method for preparing monoliths by casting metal particle suspensions.

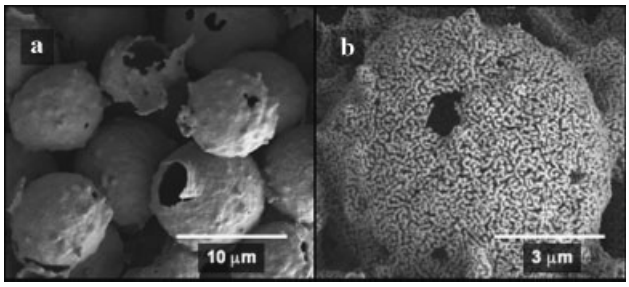

Figure 5. a) Fracture surface of a monolith containing hollow $Ag_{0.85}Au_{0.15}$ shells with a density of 0.8 g cm^{-3} before dealloying. The holes in the shell walls are presumably due to the release of organic volatiles during bakeout. b) Nanoporous hollow gold shell after dealloying. The density of the corresponding Au foam is 0.28 g cm^{-3} (1.5% of the full density of Au).

(Scheme 2). The plaster of paris facilitates the settling of particles by slowly removing the water from the suspension. This simple technique allows one to prepare millimeter-sized monolithic samples of nanoporous materials which are very homogeneous and free of larger defects (>10 μm) such as voids. As in the case of dealloying, virtually any desired sample shape can be generated by using an appropriately shaped plaster of paris cast.

The resulting nanoporous monolith consists of randomly packed metal-coated PS spheres with void spaces between individual particles. Figure 4 shows an example of such a structure obtained by filter-casting of gold-coated PS spheres with a diameter of 9.6 μm. The apparent lack of long-range order can be attributed to the relative polydispersity of the particles, high suspension concentration (≈10 wt%), and high rate of sedimentation. In context of plasmonic applications, it is important to note that the electroless plated gold films on PS beads consist of discrete Au nanoparticles, thus adding another length scale to the structure (Fig. 4b). This may have important implications as the observation of electromagentic "hot spots" in SERS experiments has been linked to junctions between nanoparticles.[39] Finally, the pure Au foam sample can be obtained by removing the PS template by a simple heat treatment in an inert atmosphere at 400 °C.

Hierachical pore structures can be realized by starting with Ag–Au-coated PS core/shell particles and adding an additional dealloying step. Such core/shell structures can be prepared by electroless deposition of silver on Au-coated PS spheres (Scheme 1). The sequence of metal deposition is important since depositing gold on silver may result in competing Ag^0/Au^{3+}galvanic and electroless deposition reduction reactions.[42,43] The Ag-to-Au ratio of the coatings can be adjusted by varying the mole ratios during plating, and typical compositions range from $Ag_{0.85}Au_{0.15}$ to $Ag_{0.7}Au_{0.3}$.[44]

Monolithic Ag–Au alloy foam samples can then be obtained by the slip-casting/annealing sequence described above. Here, the heat treatment also leads to the formation of a Ag–Au alloy. In case of the the Ag/Au system discused here, alloying is facilitated by the matching crystalline structure of Ag and Au (both face-centered cubic (fcc) with nearly identical lattice constants) and high diffusion rates of silver and gold at elevated temperatures. An example of such a structure made from 10 μm $Ag_{0.85}Au_{0.15}$ shells is shown in Figure 5a. The diameter of the shells roughly corresponds to the size of the original PS template, indicating negligable shrinkage upon template removal and good control over the feature size.

Finally, hierarchical pore structures can be generated by dealloying of Ag–Au foam samples. Here, the concentration of the nitric acid needs to be carefully adjusted to prevent cracking of the

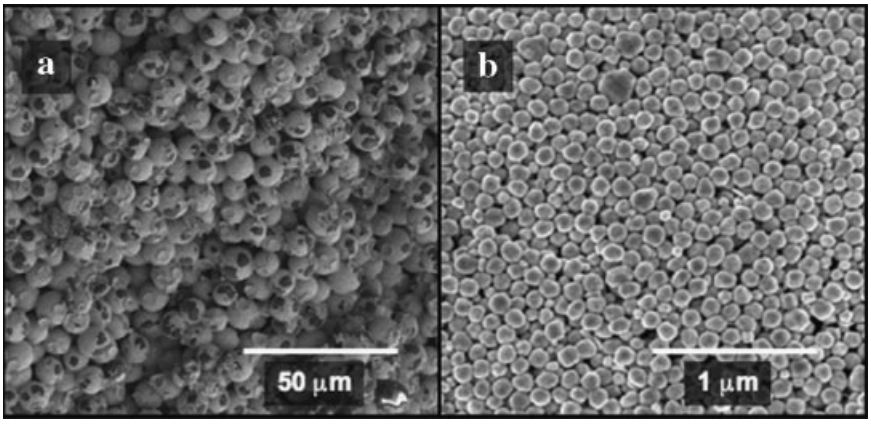

Figure 4. a) SEM image of filter-cast gold-coated PS spheres (9.6 μm diameter) fracture surface. The darker interior is the PS core, which is exposed because of surface fracture, while the lighter exterior surface is the gold surface coating. Removal of the PS template generates a pure Au foam with a density of 1.7 g cm^{-3} (~9% of the full density of Au). b) Higher-magnification SEM image of the gold coating. Note that the gold coating comprises discrete gold particles, 100–150 nm in size. The PVP stabilizer likely favors growth of individual gold particles while inhibiting gold film formation.

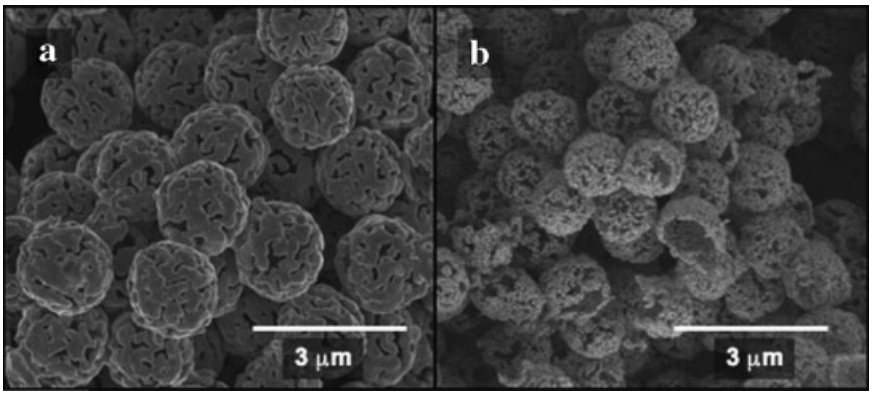

Figure 6. a) Fracture surface of a monolith containing hollow 1 μm $Ag_{0.7}Au_{0.3}$ shells before dealloying (density 1 g cm^{-3}). b) Fracture surface of a monolith containing hollow 1 μm nanoporous Au shells after dealloying (density 0.45 g cm^{-3} or 2.3% of the full density of Au).

monolithic sample. Owing to the very low density of such a material (1.5% relative density, or a void space of 98.5%), drying is challenging, particularly when one intends to make millimeter-sized samples of crack-free material. The samples need to be washed several times in distilled water to remove residual nitric acid and then placed in acetone. Once the water is completely exchanged with acetone, the monoliths can be dried by supercritical CO_2 extraction.

An SEM image of a dealloyed shell with a wall thickness of ~200 nm is shown in Figure 5b. The shell diameter (~9.6 μm) is similar to the diameter of the original template thus suggesting little volume change during dealloying and consequent drying. Thus the process outlined above provides good control over the size of the cavities. The feature size introduced by dealloying is in the range of 10–100 nm, giving rise to a relatively large surface area of ~1.5 $m^2 g^{-1}$ which is comparable to that of np Au. Thus this material combines the high surface area of np Au with the morphology control characteristic for templating techniques.

The size of the cavities only depends on the size of the orginal PS template, and consequently much smaller structures than the examples described above can be prepared. Figure 6a shows a porous Ag–Au alloy monolith obtained by slip casting 1 μm $Ag_{70}Au_{30}$ alloy shells prepared from 1 μm PS beads. The Ag–Au alloy shell is approximately 50–100 nm thick and consists of individual particles rather than a continuous film. As described above, consequent dealloying leads to the formation of a nanoporous Au foam sample with 1 μm cavities and a dealloying-induced porosity with a feature size of ~10 nm (Figure 6b).

4. Summary

We have reviewed different schemes for the generation of porous metals with well-defined pore size distributions (including complex hierarchical porosities) and adjustable densities down to a few percent of the full density. The methods described here do not result in the formation of long-range-ordered structures, but are capable of delivering homogeneous materials on a millimeter length scale. Furthermore, they provide excellent control over feature size ranging from a few nanometers up to a few micrometers, which can be exploited to tune material properties for photonic and plasmonic applications, as recently demonstrated. The technology is not only very flexible in terms of engineering new pore morphologies, but can be easily extended to generate new functional structures, for example, via using active optical materials as templates or by adding these materials during the slip-casting process.

[1] W. L. Barnes, A. Dereux, T. W. Ebbesen, *Nature* **2003**, *424*, 824.
[2] S. A. Maier, *Plasmonics: Fundamentals and Applications*, Springer, New York **2007**.
[3] S. A. Maier, H. A. Atwater, *J. Appl. Phys.* **2005**, *98*, 011101.
[4] N. Felidj, S. L. Truong, J. Aubard, G. Levi, J. R. Krenn, A. Hohenau, A. Leitner, F. R. Aussenegg, *J. Chem. Phys.* **2004**, *120*, 7141.
[5] We use the term ''metamaterials'' in a broad sense to describe the fact that the properties of the materials described here are strongly affected by their cellular architecture. In this broad sense, long-range order is not a necessary requirement.
[6] O. D. Velev, P. M. Tessier, A. M. Lenhoff, E. W. Kaler, *Nature* **1999**, *401*, 548.
[7] F. Yu, S. Ahl, A. M. Caminade, J. P. Majoral, W. Knoll, J. Erlebacher, *Anal. Chem.* **2006**, *78*, 7346.
[8] M. C. Dixon, T. A. Daniel, M. Hieda, D. M. Smilgies, M. H. W. Chan, D. L. Allara, *Langmuir* **2007**, *23*, 2414.
[9] A. I. Maaroof, A. Gentle, G. B. Smith, M. B. Cortie, *J. Phys. D: Appl. Phys.* **2007**, *40*, 5675.
[10] T. A. Kelf, Y. Sugawara, J. J. Baumberg, M. Abdelsalam, P. N. Bartlett, *Phys. Rev. Lett.* **2005**, *95*, 116802.
[11] P. M. Tessier, O. D. Velev, A. T. Kalambur, J. F. Rabolt, A. M. Lenhoff, E. W. Kaler, *J. Am. Chem. Soc.* **2000**, *122*, 9554.
[12] P. Tessier, O. D. Velev, A. T. Kalambur, A. M. Lenhoff, J. F. Rabolt, E. W. Kaler, *Adv. Mater.* **2001**, *13*, 396.
[13] S. O. Kucheyev, J. R. Hayes, J. Biener, T. Huser, C. E. Talley, A. V. Hamza, *Appl. Phys. Lett.* **2006**, *89*, 053102.
[14] V. Zielasek, B. Jurgens, C. Schulz, J. Biener, M. M. Biener, A. V. Hamza, M. Baumer, *Angew. Chem. Int. Ed.* **2006**, *45*, 8241.
[15] C. X. Xu, J. X. Su, X. H. Xu, P. P. Liu, H. J. Zhao, F. Tian, Y. Ding, *J. Am. Chem. Soc.* **2007**, *129*, 42.
[16] M. Haruta, *Chem. Phys. Chem.* **2007**, *8*, 1911.
[17] J. Biener, A. M. Hodge, J. R. Hayes, C. A. Volkert, L. A. Zepeda-Ruiz, A. V. Hamza, F. F. Abraham, *Nano Lett.* **2006**, *6*, 2379.
[18] D. Kramer, R. N. Viswanath, J. Weissmueller, *Nano Lett.* **2004**, *4*, 793.
[19] R. C. Newman, S. G. Corcoran, J. Erlebacher, M. J. Aziz, K. Sieradzki, *MRS Bull.* **1999**, *24*, 24.
[20] J. Erlebacher, M. J. Aziz, A. Karma, N. Dimitrov, K. Sieradzki, *Nature* **2001**, *410*, 450.
[21] A. M. Hodge, J. R. Hayes, J. A. Caro, J. Biener, A. V. Hamza, *Adv. Eng. Mater.* **2006**, *8*, 853.

[22] Au-richer alloys develop a self-passivating Au-rich surface layer, whereas Ag-richer alloys tend to disintegrate into a powder during dealloying.
[23] D. J. Tulimieri, J. Yoon, M. H. W. Chan, *Phys. Rev. Lett.* **1999**, *82*, 121.
[24] A. Dursun, D. V. Pugh, S. G. Corcoran, *J. Electrochem. Soc.* **2003**, *150*, B355.
[25] Y. Ding, Y. J. Kim, J. Erlebacher, *Adv. Mater.* **2004**, *16*, 1897.
[26] A. M. Hodge, J. Biener, J. R. Hayes, P. M. Bythrow, C. A. Volkert, A. V. Hamza, *Acta Mater.* **2007**, *55*, 1343.
[27] R. Li, K. Sieradzki, *Phys. Rev. Lett.* **1992**, *68*, 1168.
[28] L. H. Qian, X. Q. Yan, T. Fujita, A. Inoue, M. W. Chen, *Appl. Phys. Lett.* **2007**, *90*, 153120.
[29] Y. Ding, J. Erlebacher, *J. Am. Chem. Soc.* **2003**, *125*, 7772.
[30] K. M. Kulinowski, P. Jiang, H. Vaswani, V. L. Colvin, *Adv. Mater.* **2000**, *12*, 833.
[31] D. Walsh, L. Arcelli, T. Ikoma, J. Tanaka, S. Mann, *Nat. Mater.* **2003**, *2*, 386.
[32] G. J. D. Soler-illia, C. Sanchez, B. Lebeau, J. Patarin, *Chem. Rev.* **2002**, *102*, 4093.
[33] Y. N. Xia, B. Gates, Y. D. Yin, Y. Lu, *Adv. Mater.* **2000**, *12*, 693.
[34] G. W. Nyce, J. R. Hayes, A. V. Hamza, J. H. Satcher, *Chem. Mater.* **2007**, *19*, 344.
[35] T. Pham, J. B. Jackson, N. J. Halas, T. R. Lee, *Langmuir* **2002**, *18*, 4915.
[36] Z. J. Liang, A. Susha, F. Caruso, *Chem. Mater.* **2003**, *15*, 3176.
[37] W. L. Shi, Y. Sahoo, M. T. Swihart, P. N. Prasad, *Langmuir* **2005**, *21*, 1610.
[38] T. H. Ji, V. G. Lirtsman, Y. Avny, D. Davidov, *Adv. Mater.* **2001**, *13*, 1253.
[39] A. M. Michaels, J. Jiang, L. Brus, *J. Phys. Chem. B* **2000**, *104*, 11965.
[40] W. D. Callister, *Materials Science and Engineering: An Introduction*, 6th ed., John Wiley & Sons, New York **2003**.
[41] J. R. Hayes, G. W. Nyce, J. D. Kuntz, J. H. Satcher, A. V. Hamza, *Nanotechnology* **2007**, *18*, 275602.
[42] Y. G. Sun, Y. N. Xia, *J. Am. Chem. Soc.* **2004**, *126*, 3892.
[43] Y. G. Sun, B. T. Mayers, Y. N. Xia, *Nano Lett.* **2002**, *2*, 481–485.
[44] T. Shibata, B. A. Bunker, Z. Y. Zhang, D. Meisel, C. F. Vardeman, J. D. Gezelter, *J. Am. Chem. Soc.* **2002**, *124*, 11989.

